Jurnal Pendidikan Geografi:
Kajian, Teori, dan Praktik dalam Bidang Pendidikan dan Ilmu Geografi, 28(2), 2023, 209-227
ISSN: 0853-9251 (Print): 2527-628X (Online)
DOI: 10.17977/um017v28i22023p209-227

Seismic hazard analysis using Deterministic Seismic Hazard Analysis (DSHA) Method: A case study in Southern Malang District, East Java

Widodo Eko Prasetyo*[1], Listyo Yudha Irawan, Rudi Hartono**, Endratno Budi Santosa*****

* Intitut Teknologi Sepuluh Nopember, Sukolilo, Surabaya, East Java, 60111, Indonesia
** Universitas Negeri Malang, Semarang Street No. 5 Malang, East Java, 65141, Indonesia
*** University of Amsterdam, Roeterseilandcampus, Nieuwe Achtergracht 166, 1018 WV, Amsterdam, The Netherlands
[1]Corresponding author, Email: widodoekogeo@gmail.com

Paper received: 28-07-2022; revised: 13-04-2023; accepted: 17-05-2023

Abstract

Indonesia is a country that has a high earthquake threat. The United States Geological Survey (USGS) recorded that Indonesia experienced 5,439 earthquakes with a magnitude of Mw 5. Geologically, Indonesia is located about 200 km from the subduction zone of the Indo-Australian and Eurasian plates. Malang Regency faces the subduction of the Indo-Australian and Eurasian plates. Earthquakes that occur in plate subduction areas will propagate in various directions, including to Malang Regency. Thus, Malang Regency, especially in the southern part, has a high earthquake threat. This study aims to calculate the earthquake threat using a deterministic approach. Earthquake threats can be calculated using the Deterministic Seismic Hazard Analysis (DSHA) method. This study obtained the Mc. Guirre and Donovan attenuation function. These two attenuation functions produce different Peak Ground Acceleration values. The calculations with the Mc. Guirre attenuation function has a range of PGA values from 38,76461 gals to 69,78215 gals. Meanwhile, the Donovan attenuation function calculation produces a range of PGA values from 41.97550 gals to 76.21376 gals. Based on the value of ground acceleration during an earthquake, Bantur, Gedangan, and Sumbermanjing sub-districts are the sub-districts with the highest earthquake threat level in Southern Malang Regency. Tirtoyudo Village, Tirtoyudo District, Malang District has a lower PGA value when compared to Gedangan District. However, the amount of damage to buildings in this subdistrict was much higher. Since the building structure in Tirtoyudo Village cannot withstand ground shaking due to the earthquake, there is damage to the structure of the building.

Keywords: earthquake; Deterministic Seismic Hazard Analysis; Peak Ground Acceleration

1. Introduction

Indonesia is located at the confluence of the world's large and several small plates (Syafitri, Bahtiar, & Didik, 2020). This condition causes Indonesia to have a high threat of earthquake disasters (Imani, Arman, & Sari, 2021; Noor, 2018; Rahman & Wijayanto, 2021). A large number of earthquake disasters can prove this from 2000-2021, which reached 5,439 events. The United States Geological Survey (USGS) records that Indonesia experiences hundreds of earthquakes with a magnitude of ≥ Mw 5 every year.

The movement of the Indo-Australian plate dominates the tectonic dynamics of Java Island (Sapanji & Hamdani, 2020). The Indo-Australian plate moved relatively north, then collided with the relatively stationary Eurasian plate (Kumala, Huda, & Irawan, 2018; Linda, Ihsan, & Palloan, 2019). This tectonic activity then makes the Java Island region an active tectonic area. This is what makes Java Island have a high level of seismicity (Widagdo & Permana, 2021). Thus, the East Java Region is also experiencing active plate movement. This tectonic movement triggers an earthquake in the subduction area.

Malang District is an area that has a high threat of earthquakes (Geological Agency, 2021). Geologically, it is located about 200 km from the plate subduction zone. Earthquakes that occur in the plate subduction area will propagate in various directions. The energy of this earthquake propagation then reached the East Java Region. This is what triggers the high threat of earthquakes in Malang District.

The area of Malang District is composed of rocks of tertiary age, some of which have been weathered. In addition, Malang District also has unconsolidated quaternary deposits. These geological conditions can strengthen the effects of earthquake shocks (Geological Agency, 2021). Based on the types of rocks that compose it, the Malang area can be considered earthquake-prone because amplification can occur when seismic waves pass through the medium, resulting in stronger shocks on the surface.

The Regional Agency for Disaster Management (BPBD) of Malang Regency reported two earthquakes occurring in 2021, April 10 and April 11, with the strength of the earthquake reaching a magnitude of 6.1 and 5.5, respectively. The higher the earthquake incident, the bigger the disaster threat (Susilanto, Ngadmanto, Sunardi, & Rohadi, 2019; Yuliana & Tejakusuma, 2016). In the two times earthquake incidents, the total damage to buildings reached 10,811. The data is the total number of 13 sub-districts in the research location. Details of the amount of damage to buildings can be seen in Table 1.

Table 1. Table of the Number of Buildings Damaged by the Earthquake in Malang District

No	Subdistrict	House and Building			Total	Rank
		Minor Damage	Moderate Damage	Major Damage		
1	Tirtoyudo	1329	822	556	2707	1
2	Dampit	1174	849	381	2404	2
3	Ampelgading	1164	524	361	2049	3
4	Turen	991	316	50	1357	4
5	Sumawe	134	997	187	1318	5
6	Bantur	142	44	71	257	6
7	Gedangan	141	82	9	232	7
8	Pagak	79	50	18	147	8
9	Kepanjen	90	11	6	107	9
10	Kalipare	54	33	12	99	10
11	Gondanglegi	67	3	5	75	11
12	Donomulyo	38	8	1	47	12
13	Sumberpucung	3	7	2	12	13

Source: BPBD (2021)

Earthquake hazards can be calculated with a deterministic approach. It is done by using Deterministic Seismic Hazard Analysis (DSHA) method. It is a calculation method of Seismic Hazard Analysis by determining the ground motion parameter with the maximum earthquake magnitude and the closest distance from the source of the earthquake from the observation point (Mase, 2020; Tripathi & Zafar, 2016; Verma & Zafar, 2017). This method can be used to calculate the worst-case scenario of an earthquake hazard.

The purpose of this research is to determine the distribution of Peak Ground Acceleration (PGA) located in the southern part of Malang District, determine the earthquake hazard zone in the southern part of Malang District, and conduct a detailed scale mapping of damage to buildings due to the earthquake in the areas most affected by the earthquake on April 11 2021.

2. Method

2.1. Research Sites

This research was conducted in the southern part of Malang District. This area encompasses 12 subdistricts: 1) Donomulyo, 2) Kalipare, 3) Sumberpucung, 4) Kepanjen, 5) Pagak, 6) Bantur, 7) Gedangan, 8) Gondanglegi, 9) Turen, 10) Dampit, 11) Tirtoyudo, 12) Ampelgading. This site has the highest level of damage to buildings in Malang District.

2.2. Data Collection

This research used the secondary data obtained from several sources, namely: 1) United States Geological Survey (USGS), 2) Energy and Mineral Resources, and 3) Ina-Geoportal. As for the secondary data used, namely: 1) Earthquake catalog, 2) regional geological data, and 3) borderline. The earthquake catalog used in this research was obtained from USGS, and it includes: 1) origin time, 2) epicenter location, 3) the depth of the earthquake source, and 4) magnitude. The data details used in this study can be seen in Table 2.

Table 2. Types of Data and Data Sources

No	Data	Function	Source
1	Origin Time	Incident time	USGS
2	Epicenter Location	PGA Calculation	USGS
3	Depth	PGA Calculation	USGS
4	Magnitude	PGA Calculation	USGS
5	Area Geology	Geology Map	ESDM
6	Borderline	Borderline Map	Ina-Geoportal

The data obtained from USGS does not yet have the same type of magnitude. Therefore, before processing the data, it needs to do magnitude uniformity. This research used moment magnitude (Mw) as the uniformity basis of magnitude type. The moment magnitude (Mw) was used since the earthquake scale measurement of this magnitude type can represent the amount of energy released from the fault plane (Gunawan, Ratri, & Gunawan, 2020; Latifa, Meiliyadi, & Bahtiar, 2022; National Agency for Disaster Management Australia-Indonesia Facility for Disaster Reduction, 2010; Pasau, Bobanto, & Pandara, 2018; Somantri, 2021). Further, the magnitude conversion was done by using the attached formula in Table 3.

Table 3. Magnitude Conversion Formula

No	Conversion Correlation	Data Range
1	Mw = 0,143*Ms – 1,051*Ms + 7,285	4,5 ≤ Ms ≤ 8,6
2	Mw = 0,114*Mb – 0,556*Mb + 5,560	4,9 ≤ Mb ≤ 8,2
3	Mw = 0,787*Me + 1,537	5,2 ≤ Me ≤ 7,3
4	Mb = 0,125*Ml^2 – 0.389*Ml + 3,513	3,0 ≤ Ml ≤ 6,2
5	ML = 0,717*Md + 1,003	3,0 ≤ Md ≤ 5,8

Source: The National Center for Earthquake Studies (2017)

This research limits on the earthquake magnitude is used. The earthquake used in this study is an earthquake which has Mw ≥ 5 magnitude. This limit is done to avoid underestimated calculation results. The earthquake of Mw ≥ 5 magnitude was chosen as a limitation based on the consideration that earthquakes with a strength of Mw ≥ 5 can have a significant impact on vibrations on the earth's surface and the resilience of building infrastructure (Pangaribuan, Rasimeng, Karyanto, & Rudianto, 2019). In addition, this research used earthquake data for the period 1958 to 2021.

2.3. Data Analysis Technique

The data analysis was done by using a deterministic approach. It was conducted by designing a certain earthquake scenario on the bedrock. It was formed by taking into account the earthquake that occurred at a certain location in a certain earthquake magnitude (Naik & Choudhury, 2015; Salsabil, Hilyah, Purwanto, & Fajar, 2018). Further, the deterministic approach is an applicable approach to be conducted to predict the ground motion which was caused by an earthquake (Patel, Solanki, & Thaker, 2022; Resta, Apriliyani, Nasri, & Dewi, 2021). Although it is applicable, the deterministic approach has flaws where it only focuses on the distance and magnitude of the earthquake, while the influence of the uncertainty of the earthquake is not considered (National Agency for Disaster Management Australia-Indonesia Facility for Disaster Reduction, 2010; Salsabil et al., 2018).

The DSHA analysis includes decisions and subjective opinions from relevant experts in determining the potential for an earthquake. Consequently, the experts have different perspectives from one another. This difference caused them difficulty agreeing on the earthquake potential (Sunardi & Sulastri, 2016; Utomo & Wahyudi, 2017). The powerless to make an agreement makes each expert have different formulas and constants in their calculations. Additionally, the DSHA calculation in this study used attenuation functions: 1) Mc. Guirre, and 2) Donovan.

Mc. Guire: $$E[v] = a.10^{bM}(R + 25)^{-c} \quad (1)$$

Donovan: $$y = b_1.e^{b_2.M}(R + 25)^{-b_3} \quad (2)$$

Description:
E = Expectation
v = in gal
a = 472
b = 0.278
M = Magnitude Surface (Ms)
R =Distance between two points in units equivalent to the radius of the Earth
C = 1.301
y = *in gal*
b_1 = 1080
b_2 = 0.5
b_3 = 1.32
e = 10

$$R = \sqrt{X^2 + hypocenter^2} \quad (3)$$

$$X = \sqrt{((x - x_1)^2 + (y - y_1)^2).CF} \quad (4)$$

Description:

X	= Distance between two points in two-dimensional Cartesian coordinates with scale factor CF
(x, y)	= represents the coordinates of a point
(x_1, y_1)	= represents the coordinates of a reference point
Constant Factor (CF)	= 111

2.4. Peak Ground Acceleration (PGA)

The acceleration is a parameter used to state the change in the object's speed from rest to a certain speed regardless of direction (Pakuani & Kurniawan, 2021; Suwandi, Sari, & Waslaluddin, 2017). The Peak Ground Acceleration (PGA) is the largest ground vibration acceleration value that has ever occurred in an area due to the propagation of earthquake waves (Hason, Hanoon, & Abdulhameed, 2021; Salahshoor, Lyubushin, Shabani, & Kazemian, 2018). The maximum PGA that was done at a certain point due to the earthquake can be calculated by seeing the magnitude and hypocenter distance and the predominant period of soil where it was located (Palupi, Raharjo, & Alfiani, 2020).

Moreover, the PGA outcome could indicate the earthquake threat in a certain place (Hsu, Wu, Liang, Kuo, & Lin, 2020; Shiuly, 2018). The PGA value is directly proportional to the threat of earthquakes in the region. In other words, the greater the PGA value that has occurred in a place, the greater the threat of an earthquake that may occur (Dari & Pujiastuti, 2021; Pakpahan, Tambunan, Mannesa, & Tambunan, 2021). It happened because the higher the PGA score, the greater the acceleration of ground vibrations in that region (Aditama & Fatimah, 2020). Thus, with a high PGA value, the primary effects of earthquakes will also be higher (Halimatusadiyah, Suryanita, & Yusa, 2021). The primary effect of earthquake is the effect of direct earthquake (Setyorini, 2020). This effect includes: 1) building structures damage, 2) fallen tree, 3) landslide, and 4) others. This damage was caused by the earthquake vibrations generated (Sungkowo, 2016).

In addition, the PGA values can be expressed in terms of g (gravitational acceleration = g) or cm/second square (1 g = 9,81 cm/s^2). Moreover, PGA could also be stated as gals where 1 gals equals 0.01 cm/second square (1 G = 981 gals). The PGA determination using equations is not always correct and has different methods for each equation depending on the parameters used. The PGA value at a certain point is also influenced by the geological structure of the area from the research point (Aditama & Fatimah, 2020; Murdiantoro, Sismanto, & Marjiyono, 2018). In addition to the geological structure, the PGA value is also influenced by the hypocenter distance. The closer an area is to the source of the earthquake, the greater the acceleration of the ground surface in that area (Douglas, 2002). The research flowchart is presented in Figure 1.

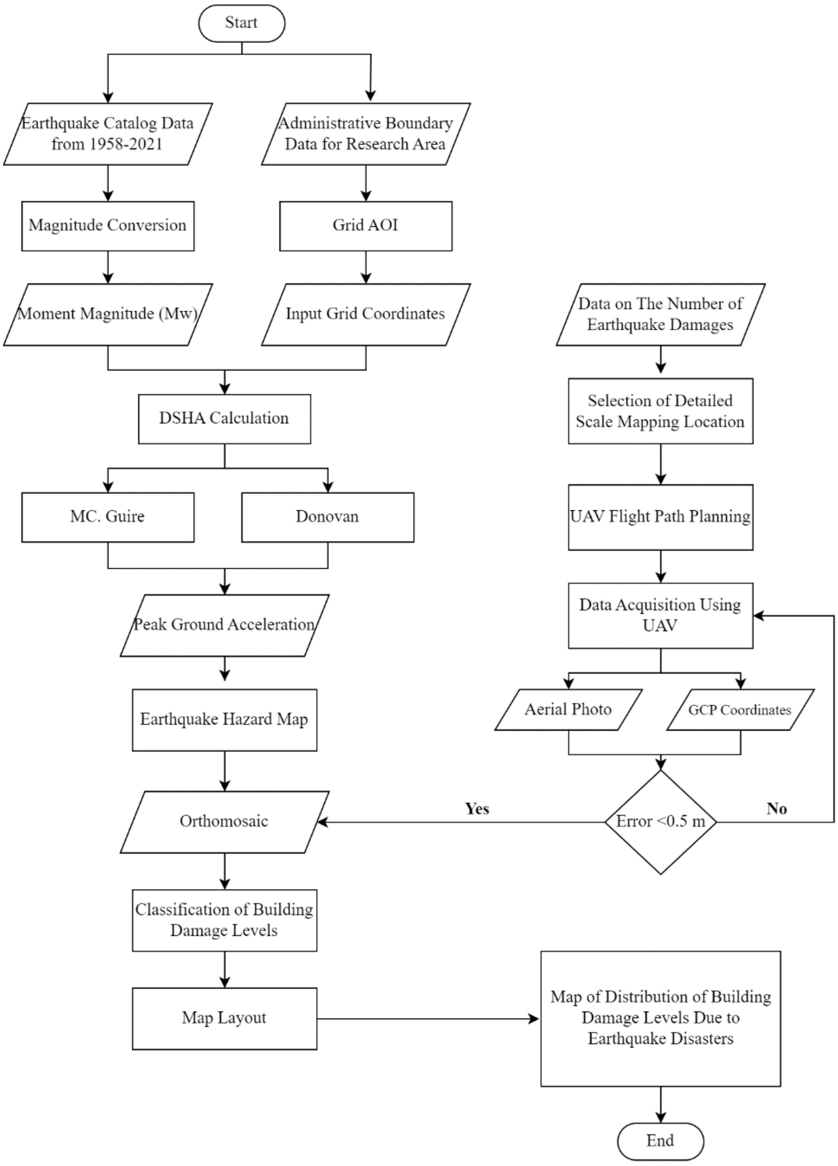

Figure 1. Research Flowchart

3. Results and Discussion

3.1. Geological Area of the Southern Part of Malang

The geological area of the southern part of Malang is dominated by Quaternary, Neogene, and Paleogene rocks. There are seventeen types of geology located in the southern part of Malang, consisting of Qal, Qas, Qlks, Qlv, Qpj, Qpkb, Qpvb, Qvj, Qvk, Qvs, Qvtm, Tmn, Tmw, Tmwl, Tomi, Tomm, Tomt. The geological difference led to the differences in dispersed rock materials. Different rock materials will give different responses and impacts when transmitted by earthquake waves (Giang, Pham, & Nguyen, 2022; Pirhadi, Tang, & Yang, 2019). This difference can occur due to differences in the level of rock cohesiveness, density, and rock strength (Karimzadeh, Feizizadeh, & Matsuoka, 2017; Maringue et al., 2022). Paleogene-aged rocks have material that is loose, not solid, and not compact (Fasulo & Ridgway, 2021; Jamil, Rahman, Siddiqui, Ibrahim, & Ahmed, 2020; Nicholson, Bray, Gulick, & Aduomahor, 2022). Therefore, when exposed to energy from earthquake waves, the material will be easily moved.

The southern part of Malang district has an active minor fault. The existence of a minor fault can trigger a high peak ground acceleration in the surrounding area when an earthquake wave passes through the fault. Based on the geological map of the area, this location has four active minor faults that are scattered in the eastern part. Geologically, the existence of the active minor fault located in the southeast of Malang causes this area to have a higher threat of earthquake disasters compared to areas that do not have minor faults. Thus, the western part has a lower threat of earthquake disasters when compared to the eastern part. A geology map of southern Malang can be found in Figure 2.

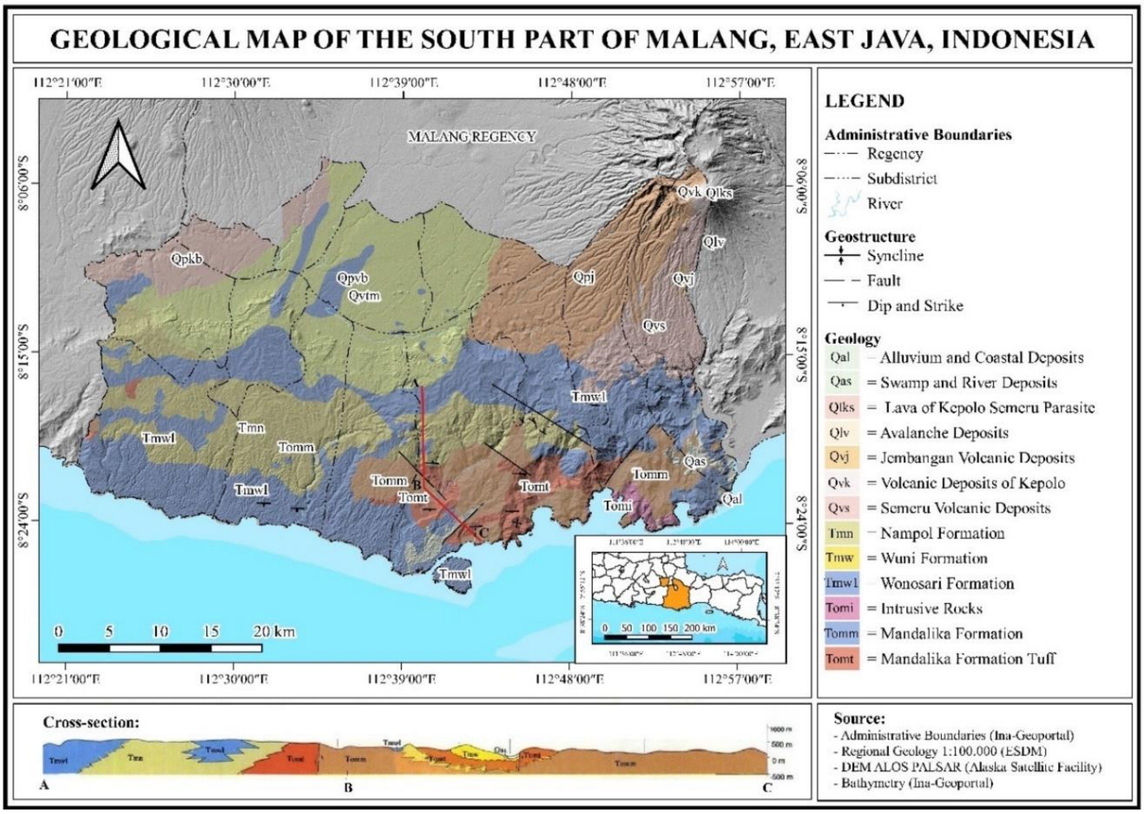

Figure 2. Geological Map

3.2. Analysis of *Peak Ground Acceleration* (PGA) in Southern Malang District

PGA values in the southern Malang District vary. It is due to the extent of the area (Abbasnejadfard, Bastami, & Fallah, 2021; Yao, Qi, Liu, & Guo, 2021). According to the analysis results, it was distinguished that Gedangan, Bantur, and Sumbermanjing Subdistricts are the area with the highest PGA values. The PGA values of Gedangan District are on coordinate -8.394S, 112.604E, which has the value 0.07575 g for the Donovan attenuation function and the same value for the Mc. Guirre attenuation function. Further, the ground motion acceleration in Gedangan District reaches 0.74282 m/s2 for the Donovan attenuation function and 0.68038 m/s^2 for the Mc.Guirre attenuation function. Besides, Turen subdistrict is an area that has the lowest PGA value than other subdistricts in the Southern part of Malang District. It was found that Turen District at coordinates -8.168S, 112.694E has a PGA value of 0.05627 in g and

0.55184 m/s^2 for calculations using the Donovan attenuation function. Meanwhile, the PGA values for Turen District using the attenuation function of McGuirre are 0.05176 g and 0.50763 m/s^2. Peak Ground Acceleration (PGA) values for each sub-district can be seen in Table 4.

Table 4. Peak Ground Acceleration Value in Each District

Subdistrict	Coordinate		*Peak Ground Acceleration*			
	Longitude	Latitude	Donovan (g)	Mc. Guirre (g)	Donovan (m/s^2)	Mc. Guirre (m/s^2)
Sumberpucung	-8.169	112.513	0.05666	0.05212	0.55569	0.51112
Kepanjen	-8.168	112.558	0.05736	0.05275	0.56248	0.51727
Turen	-8.168	112.694	0.05627	0.05176	0.55184	0.50763
Kalipare	-8.214	112.422	0.05713	0.05254	0.56022	0.51522
Gondanglegi	-8.213	112.649	0.06095	0.05600	0.59774	0.54921
Pagak	-8.259	112.513	0.06412	0.05887	0.62882	0.57735
Dampit	-8.258	112.785	0.05936	0.05456	0.58216	0.53510
Donomulyo	-8.350	112.423	0.06600	0.06058	0.64727	0.59404
Ampelgading	-8.348	112.922	0.05460	0.05025	0.53545	0.49276
Bantur	-8.395	112.514	0.07383	0.06765	0.72402	0.66341
Gedangan	-8.394	112.604	0.07575	0.06938	0.74282	0.68038
Sumbermanjing	-8.394	112.695	0.07297	0.06687	0.71561	0.65581
Tirtoyudho	-8.393	112.877	0.05947	0.05466	0.58317	0.53602

The gals' PGA value of each subdistrict also varies (Işık, Büyüksaraç, Ekinci, Aydın, & Harirchian, 2020; Khoshnevis, Taborda, Azizzadeh-Roodpish, & Cramer, 2017). Gedangan subdistrict in coordinate -8.394S, 112.604E has PGA value as much as 74.28163 gals for the Donovan attenuation function and 68.03822 gals for the Mc. Guire attenuation function. Turen subdistrict in the coordinate -8.168S, 112.694E has PGA value 55.18416 gals for the Donovan attenuation function and 50.76258 gals for the Mc. Guirre attenuation function. Furthermore, the PGA values in gals can be seen in Table 5.

Table 5. Value of Peak Ground Acceleration (gals) in Each District

District	Coordinate		PGA (gals)	
	Longitude	Latitude	Donovan	Mc. Guirre
Sumberpucung	-8.169	112.513	55.56935	51.11179
Kepanjen	-8.168	112.558	56.24823	51.72717
Turen	-8.168	112.694	55.18416	50.76258
Kalipare	-8.214	112.422	56.02242	51.52250
Gondanglegi	-8.213	112.649	59.77361	54.92111
Pagak	-8.259	112.513	62.88226	57.73525
Dampit	-8.258	112.785	58.21558	53.50991
Donomulyo	-8.350	112.423	64.72697	59.40425
Ampelgading	-8.348	112.922	53.54538	49.27648
Bantur	-8.395	112.514	72.40224	66.34126
Gedangan	-8.394	112.604	74.28163	68.03822
Sumbermanjing	-8.394	112.695	71.56083	65.58131
Tirtoyudho	-8.393	112.877	58.31669	53.60151

The result of the attenuation function gains different calculations (Bradley, Cubrinovski, & Wentz, 2022; Hamdy, Gaber, Abdalzaher, & Elhadidy, 2022). Donovan attenuation function has the PGA value range 41.97550 gals – 76.21376 gals. Meanwhile, the PGA value for Mc. Guire attenuation function ranges from 38.76461 gals - 69.78215 gals. The minimum and maximum calculation values can be seen in Table 6.

Table 6. Min and Max Peak Ground Acceleration Values for Each Attenuation Function

No	Method	Peak Ground Acceleration (gals)		
		Min	Average	Max
1	Donovan	41.97550	58.58002	76.21376
2	Mc.Guirre	38.76461	54.16786	69.78215

The minimum value is obtained from calculating locations that are far from the epicenter, while the maximum value is obtained from calculations at locations close to the epicenter (Gandomi, Soltanpour, Zolfaghari, & Gandomi, 2016; Hason et al., 2021). In the deterministic approach, the results obtained were influenced by the distance of the earthquake hypocenter from the research location and the magnitude of the earthquake (Caccavale, Sacchi, Spiga, & Porfido, 2019; Concha et al., 2020; Pouryari, Mahboobi Ardakani, & Hassani, 2022). Therefore, the farthest location from the earthquake will have a small PGA value, while the closest location will have a great PGA value (Kowsari, Ghazi, Kijko, Javadi, & Shabani, 2021; Mehta & Thaker, 2022; Stewart, Luco, Hooper, & Crouse, 2020). In other words, the closer a location is to the earthquake hypocenter, the greater the PGA value (Douglas, 2002; Mendoza, Ramos, & Dimalanta, 2022).

According to the calculations of Donovan and Mc. Guire formula, it was revealed that the results of both formulas have a difference. The maximum and minimum values from the calculation of the Donovan attenuation function have a greater value when compared to the results calculated using the Mc. Guirre attenuation function (Sari & Rahmatullah, 2021; Sung, Abrahamson, & Huang, 2021). In its application in Southern Malang District, Donovan's attenuation function is closer to the actual value. It is shown in the calculation results at coordinates -8.347S 112.59E. The calculation of the Donovan attenuation function at these coordinates produces a value of 71.26312 gals. This value is close to the actual value, where the PGA value at that coordinate is 75.1738 gals. At the same time, the value for the calculation uses the Mc. Guirre attenuation function on the coordinates -8.347S 112.59E is 65.31240 gals. The real PGA value can be obtained by taking the field measurement using the accelerometer.

3.3. Earthquake Hazard Map

The map of earthquake threat is designed according to the PGA value. The more the PGA value, the greater the acceleration of the ground vibrations caused by an earthquake (Tauhidur & Chhangte, 2021). The greater the ground acceleration, the greater the shock caused by the earthquake (Gogoi, Baruah, & Sharma, 2023; Wibowo & Sembri, 2016). Thus, the threat of earthquakes in the area is also getting bigger. The distribution and variation of PGA values will affect the level of earthquake threat in an area.

3.3.1. Earthquake Hazard Map with M.Guirre Attenuation Function Approach

The PGA value with Mc. Guirre attenuation function is then visualized in the form of earthquake hazard map. Additionally, the distribution of PGA values with the Mc.Guirre attenuation function greatly affects the earthquake hazard (Ulfiana, Rumy, Pratama, & Ariy, 2018; Zera, Fauziah, Nafian, & Ramadhani, 2022). The earthquake hazard map with the Mc. Guirre attenuation function approach can be seen in Figure 3.

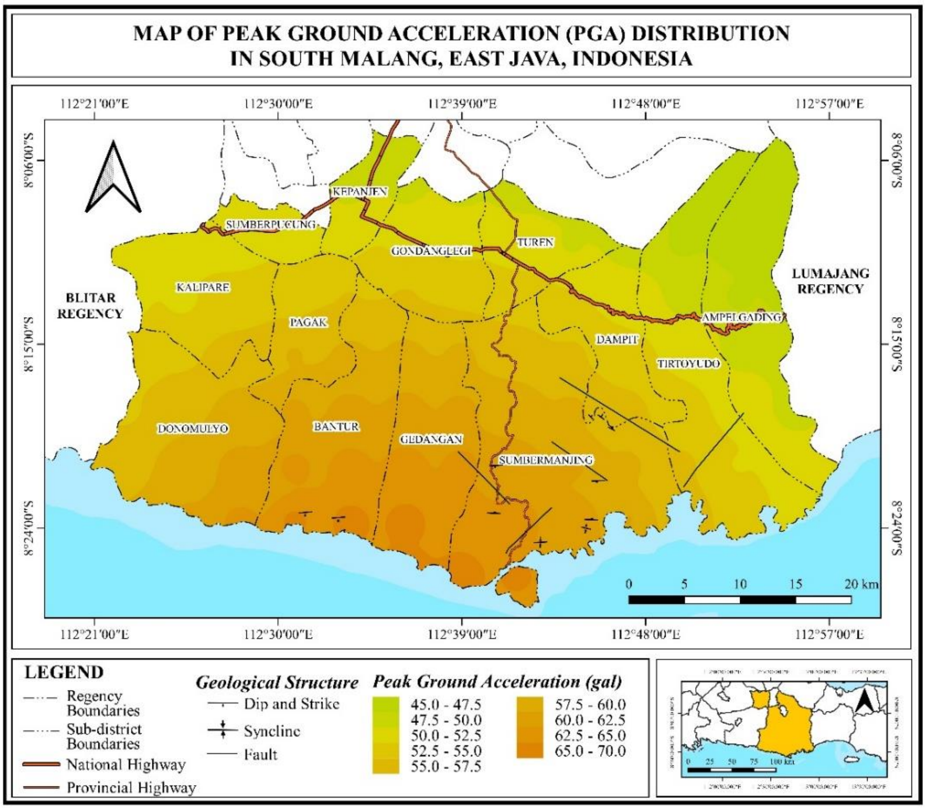

Figure 3. Peak Ground Acceleration Spread Map in Southern Part of Malang District

According to the earthquake hazard map in the southern part of Malang District, it was discovered that Bantur, Gedangan, and Sumbermanjing Subdistricts are the places with a high threat of earthquake disaster. These three subdistricts have a zone with ground acceleration with a variation 52.5–76.2 gals. These three subdistricts are directly adjacent to the sea, so this area meets the subduction of the Indo-Australian and Eurasian plates. In addition, Donomulyo, Tirtoyudho, and Ampelgading Subdistricts are also directly adjacent to the sea. However, Bantur, Gedangan, and Sumbermanjing Subdistricts have more indented structures into the sea. It brings them closer to the earthquake source. The magnitude of the earthquake threat in these areas is strongly influenced by the distance from the earthquake source, where the three subdistricts have the closest distance to the subduction of the Indo-Australian and Eurasian plates.

Besides, the other subdistricts which are further away from the earthquake source have smaller variations in PGA values. Kalipare, Sumberpucung, Kepanjen, Gondanglegi, Turen, Dampit, Tirtoyudo, and Ampelgading Subdistricts have PGA value variations 45–55 gals. Based on the value of ground movement acceleration, the threat of earthquakes in this area is smaller when compared to the Bantur, Gedangan, and Sumbermanjing Districts.

Further, according to the earthquake hazard map with Mc. Guirre attenuation, Southern part of Malang District is dominated by the ground movement acceleration value of 55.1–57.5 gals reaching 28,589.06 Ha or 18.09% of the total area. The second position is occupied by a PGA value of 57.6–60 gals with an area of 24,398.64 Ha or 15.78% of the total area. In contrast, the area with the lowest PGA value is 47.6–50 gals which only has an area of 14,928.84 Ha or

2.84% of the total area (The National Center for Earthquake Studies, 2017). Details of the area of PGA values with the Mc. Guirre attenuation function can be seen in Table 7.

Table 7. Table of Areas for Each PGA Value

PGA Value (gals)	Area (Ha)	Percentage (%)
45 - 47.5	10910.27	3.783435398
47.6 - 50	14928.84	2.843284014
50.1 - 52.5	37048.42	3.546349253
52.6 - 55	31785.42	12.92863825
55.1 - 57.5	28589.06	18.08732549
57.6 - 60	24398.64	15.773672
60.1 - 62.5	20563.35	14.08630653
62.6 - 65	15951.83	12.64846977
65.1 - 70	3851.56	10.96589247
Total	188027.39	100%

3.3.2. Earthquake Hazard Map with Donovan Attenuation Function Approach

The approach to earthquake hazard map is different between Mc. Guirre and Donovan attenuation function since both have different earthquake potential constants, making different results. The earthquake hazard map is also different, with a distribution of PGA values. Besides, the Earthquake Hazard Map with the Donovan attenuation function approach can be seen in Figure 4.

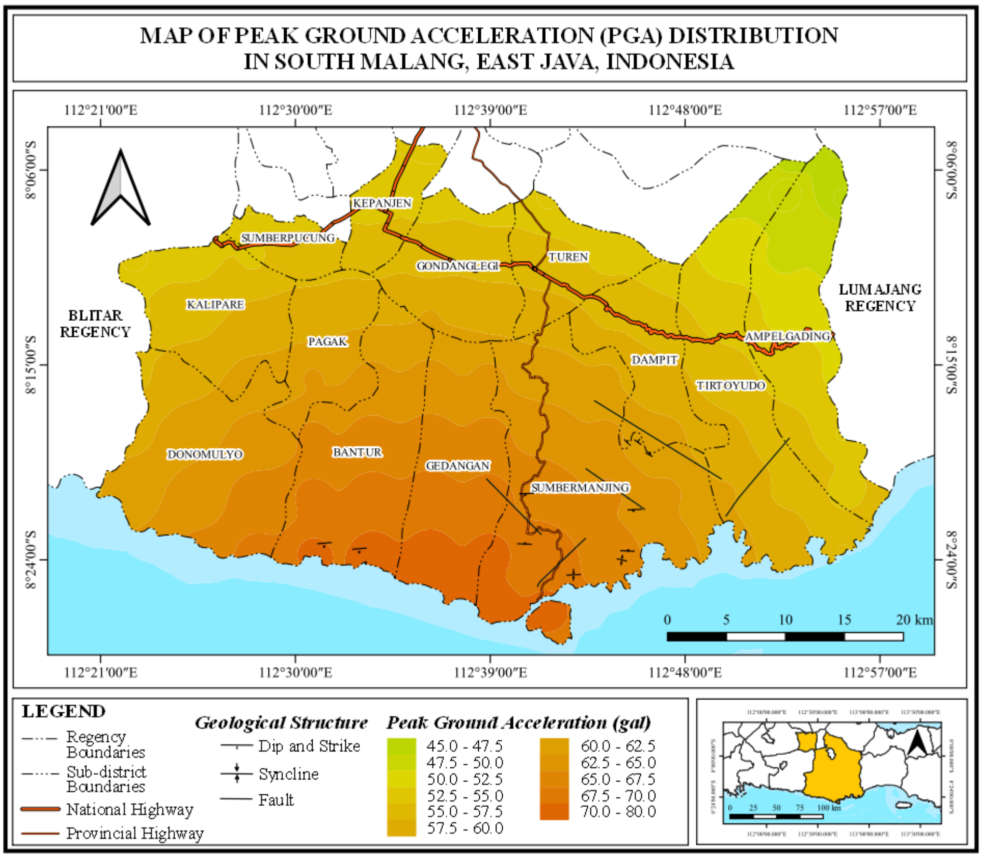

Figure 4. Peak Ground Acceleration Distribution Map in the Southern Part of Malang District

Bantur, Gedangan, and Sumbermanjing Subdistricts are still the three subdistricts with the highest earthquake threat level. However, it is different from the earthquake threat map with Mc. Guirre attenuation function, which has PGA variation range of 57.5–80 gals. The ground acceleration value in Donomulyo District is also different. In Donomulyo, it has value variations of 50.0–70.0 gals. Based on this value, Donomulyo District has a higher earthquake hazard when compared to the earthquake hazard map using Mc. Guirre attenuation function.

Meanwhile, even though Kalipare, Pagak, Sumberpucung, Kepanjen, Gondanglegi, Turen, Dampit, Tirtoyudo, and Ampelgading Districts have lower earthquake threats, the ground acceleration value in this area is still higher when compared to the ground acceleration using the Mc. Guirre attenuation function. Accordingly, this area has a peak ground acceleration variation of 45.0–60.0 gals. Otherwise, using the Donovan attenuation function, this area has a ground acceleration variation of 45.0–65.0 gals. Thus, the earthquake hazard level using the Donovan attenuation function is higher when compared to the earthquake hazard level using the Mc.Guirre attenuation function.

The southern subdistricts of Malang were dominated by PGA value 55.1–57.5 gals, which the large reached 32.562,14 Ha or 18.09% of the total area. In the meantime, the PGA value 67.7–70.0 gals be the value with the least area, namely 1490.37 Ha or 0.83% of the total area. Further, PGA value 70.1–80 gals has an area of 8,117.02 Ha or 4.5% of the total area. Although the area with a PGA value of 67.6-80 gals only covers 5.32%, this area is an area with the highest threat of earthquakes in the Southern Malang Region. Details of the area of PGA values with the Donovan attenuation function can be seen in Table 8.

Table 8. Table of Areas for Each PGA Value

PGA Value (gals)	Area (Ha)	Percentage (%)
45 - 47.5	6811.22	3.783435398
47.6 - 50	5118.69	2.843284014
50.1 - 52.5	6384.4	3.546349253
52.6 - 55	23275.09	12.92863825
55.1 - 57.5	32562.14	18.08732549
57.6 - 60	28396.93	15.773672
60.1 - 62.5	25359.21	14.08630653
62.6 - 65	22770.71	12.64846977
65.1 - 67.5	19741.61	10.96589247
67.6 - 70	1490.37	0.827857361
70.1- 80	8117.02	4.508769471
Total	180027.39	100%

Based on the calculation results, the earthquake hazard map using the Donovan attenuation function has better accuracy when compared to the Mc. Guirre attenuation function. This is based on the peak ground acceleration value with the Donovan attenuation function closer to the actual peak acceleration value (Ahnan & Agung, 2021; Anugrayanti, Arsyad, & Tiwow, 2021; Ariani, 2020; Suwandi et al., 2017). The peak ground acceleration value obtained using the accelerometer at coordinates -8.347S, 112.59E is 75.1738 gals (Sinadinovski, Pekevski, Dojcinovski, & Cernih, 2018). This value is only 3.9106 gals greater than the results calculated using the Donovan attenuation function at these coordinates. While calculations using the attenuation function have a difference of 9.8614 gals. Thus the earthquake hazard distribution map using the Donovan attenuation function is more accurate when compared to the Mc. Guirre attenuation function when applied to the Southern part of Malang District.

3.4. Level of Damage to Buildings Due to Earthquakes in Research Fields

The subdistricts in the Southern part of Malang Regency have almost the same damage but with different amounts for each sub-district. In general, building damage is caused by the inability of building structures to withstand ground vibrations caused by earthquakes (Erdogan & Yilmaz, 2019; Wang et al., 2016). Building damage was identified into three classes: 1) Minor Damage, 2) Moderate Damage, and 3) Major Damage. Details of the level of damage to buildings can be seen in Table 9.

Table 9. Level of Damage to Buildings

No	Straightforward Description	Detailed Description
1	Minor Damage	Hairline cracks on the walls, the tiles shifted down, and some fell off
2	Moderate Damage	Many cracks occurred in the walls of simple buildings, some collapsed, broken glass and plaster walls. Some were loose, and most of the tiles shifted down or fell. The building structure suffered light to moderate damage
3	Major Damage	Most of the walls of the permanent buildings collapsed. The building structure suffered heavy damage

Source: BMKG (2021)

Based on this classification, it is possible to classify the level of damage to buildings in each sub-district at the research location. By conducting a survey, it can be seen that each sub-district has three levels of damage, from minor damage to major damage. Documentation sampling was carried out at each level of damage to buildings in each district. Documentation of the level of damage to buildings in each of the three districts with the highest amount of damage can be seen in Table 10.

3.5. Application of Detailed Post-Earthquake Damage Scale Mapping in Tirtoyudo Village

Detailed scale mapping, also known as microscale mapping, is carried out to map the damage after the earthquake with a magnitude of 6.1 on April 10, 2021, and a magnitude of 5.5 on April 11, 2021. Based on data from BPBD Malang Regency, Tirtoyudo Village is one of the villages with the highest amount of building damage. According to this, Microscale Mapping was carried out to determine the distribution of the level of damage to buildings in Tirtoyudo Village.

Data acquisition is done using UAV, the data is then visualized into a map. Based on the data acquisition result map, it can be seen that the damage to buildings in Tirtoyudo Village is almost evenly distributed. Light damage to buildings is the level of damage with the largest number of houses. Then, it was followed by moderate and severe levels of damage. The building damage map can be seen in Figure 5.

Table 10. Documentation of the Level of Damage to Buildings in Each District

No	Subdistrict	Level of Damage to Buildings		
		Minor Damage	Moderate Damage	Major Damage
1	Tirtoyudo			
2	Dampit			
3	Ampelgading			

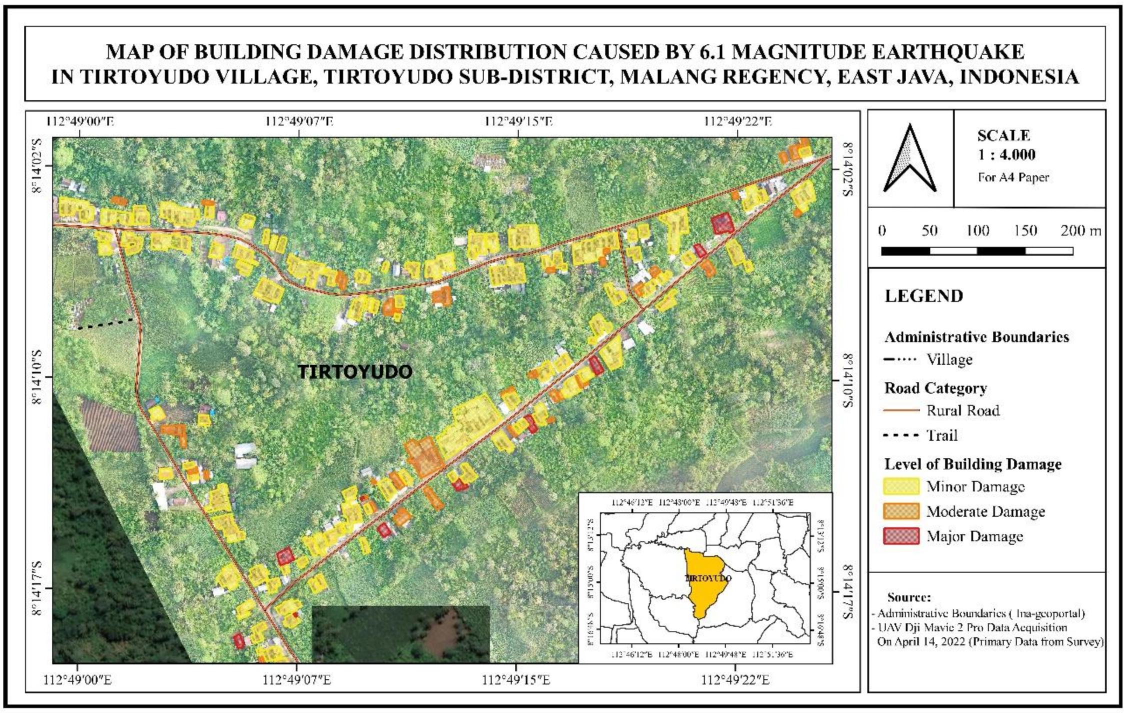

Figure 5. Map of Distribution of Levels of Damage to Buildings Due to the Earthquake

Based on the PGA value, this area has a smaller ground acceleration value than Gedangan District, which has a PGA value of 74.28163 gals. Tirtoyudho District only has a ground acceleration of 58.31669 gals. Based on this value, Tirtoyudo District, especially Tirtoyudo Village, should have a smaller threat of earthquakes. However, the amount of damage in

Tirtoyudo District was far greater than that in Gedangan District, namely, 2707 damages, while Gedangan District only amounted to 232 damages. The damage was caused by the fact that in the village of Tirtoyudho, almost all were permanent buildings made of bricks. Buildings made of wood are rare. Based on the survey results, only two buildings were made of wood. Buildings made of wood have a good ability to respond to ground vibrations, so they are more resistant to earthquakes (Alih & Vafaei, 2019; Hariyanto, Triyadib, & Widyowijatnoko, 2022; Queirós, Calejo Rodrigues, & Pereira, 2016; Sugino, Tanishima, Tanaka, Kashiwa, & Hayashi, 2022). In addition, based on interviews conducted with stakeholders, this can happen because of the building structure. Communities build buildings without regard to their resistance to earthquakes. Thus, when an earthquake occurs, the building structure cannot withstand the ground's vibrations, resulting in damage.

4. Conclusion

Southern Malang District has varying Peak Ground Acceleration (PGA) values. These variations are different for each attenuation function. Mc. Guirre attenuation function has a variety of PGA values from 38.76461 gals to 69.78215 gals. The Donovan attenuation function varies from 41.97550 gals to 76.21376 gals. The calculated value with the Donovan attenuation function is closer to the actual ground acceleration value. The PGA value with the Donovan attenuation function only has a difference of 3.9106 gals with the accelerometer measurement results. Based on the PGA value, the Southern part of Malang Regency has various earthquake threats. The sub-districts with the highest threat of earthquakes are Bantur, Gedangan, and Sumbermanjing Subdistricts. They have the shape of an area that juts into the sea. Thus, these three districts are the districts closest to the subduction of the Indo-Australian and Eurasian Plates, where the plate's subduction is one of the main sources of earthquakes. Tirtoyudo District has a lower PGA value compared to Gedangan District. However, the Tirtoyudo District had a much larger amount of damage, namely 2707 damage. This is because the building structures in Tirtoyudo District cannot withstand the ground shaking caused by the earthquake, so the buildings are damaged. Other subdistricts also experienced similar damage, although not as much as the amount of damage in Tirtoyudo Subdistrict.

References

Abbasnejadfard, M., Bastami, M., & Fallah, A. (2021). Investigating the spatial correlations in univariate random fields of peak ground velocity and peak ground displacement considering anisotropy. *Geoenvironmental Disasters*, *8*, 1–16.

Aditama, T., & Fatimah, F. (2020). Peran data mikroseismik dan geologi untuk analisis potensi longsor Daerah Cinomati, Kecamatan Pleret–Dlingo, Kabupaten Bantul, Daerah Istimewa Yogyakarta. *GEODA*, *1*(2), 95–104.

Ahnan, M., & Agung, P. A. M. (2021). Settlement of geosynthetic encased stone columns liquefaction condition in box culvert. *Logic: Jurnal Rancang Bangun dan Teknologi*, *21*(1), 40–51.

Alih, S. C., & Vafaei, M. (2019). Performance of reinforced concrete buildings and wooden structures during the 2015 Mw 6.0 Sabah earthquake in Malaysia. *Engineering Failure Analysis*, *102*, 351–368.

Anugrayanti, A., Arsyad, M., & Tiwow, V. A. (2021). Analysis of susceptible disaster region based on the peak ground acceleration and earthquake intensity in Mamasa 2018. *Journal of Physics: Conference Series*, *1816*(1), 12014. IOP Publishing.

Ariani, E. (2020). Analysis of a peak ground acceleration value and earthquake intensity using Donovan Method in Banten Province. *Spektra: Jurnal Fisika dan Aplikasinya*, *5*(3), 213–220.

BMKG. (2021). *Earthquake intensity scale BMKG*. Retrieved from bmkg.go.id website: https://-www.bmkg.go.id/gempabumi/skala-intensitas-gempabumi.bmkg

BPBD. (2021). *Number and level of building damages due to earthquake in April 2021 in Malang Regency*. Malang.

Bradley, B., Cubrinovski, M., & Wentz, F. (2022). Probabilistic seismic hazard analysis of peak ground acceleration for major regional New Zealand locations. *Bulletin of the New Zealand Society for Earthquake Engineering*, *55*(1), 15–24.

Caccavale, M., Sacchi, M., Spiga, E., & Porfido, S. (2019). The 1976 Guatemala earthquake: ESI scale and Probabilistic/Deterministic seismic hazard analysis approaches. *Geosciences*, *9*(9), 403.

Concha, N., Guinto, J., Grimaldo, A., Espinoza, M., Juan, D., & Mapacpac, M. (2020). A deterministic approach of generating earthquake liquefaction severity map of Mindoro, Philippines. *GEOMATE Journal*, *18*(70), 94–98.

Dari, R. W., & Pujiastuti, D. (2021). Studi bahaya seismik dengan metode probabilistic seismic hazard analisys di Kabupaten Mentawai. *Jurnal Fisika Unand*, *10*(4), 532–539.

Douglas, J. (2002). Note on scaling of peak ground acceleration and peak ground velocity with magnitude. *Geophysical Journal International*, *148*(2), 336–339.

Erdogan, M., & Yilmaz, A. (2019). Detection of building damage caused by Van Earthquake using image and Digital Surface Model (DSM) difference. *International Journal of Remote Sensing*, *40*(10), 3772–3786.

Fasulo, C. R., & Ridgway, K. D. (2021). Detrital zircon geochronology of modern river sediment in south-central Alaska: Provenance, magmatic, and tectonic insights into the Mesozoic and Cenozoic development of the Southern Alaska convergent margin. *Geosphere*, *17*(4), 1248–1267.

Gandomi, M., Soltanpour, M., Zolfaghari, M. R., & Gandomi, A. H. (2016). Prediction of peak ground acceleration of Iran's tectonic regions using a hybrid soft computing technique. *Geoscience Frontiers*, *7*(1), 75–82.

Geological Agency. (2021). *Kebencanaan geologi*. Ministry of Energy and Mineral Resources.

Giang, K. T., Pham, D. N., & Nguyen, D. V. (2022). Effect of local site conditions on earthquake ground motions in Hanoi: Results from numerical simulations. *VNU Journal of Science: Mathematics-Physics*, *38*(2), 82–90.

Gogoi, A., Baruah, S., & Sharma, S. (2023). Regression analysis on ground motion parameters for the earthquakes (Mw≥ 4.0) in NE India with special emphasis on 3 Jan 2016 M6. 7, Tamenglong earthquake. *Physics and Chemistry of the Earth, Parts A/B/C*, *129*, 103316.

Gunawan, T., Ratri, A. D. P., & Gunawan, M. T. (2020). Studi karakteristik gempabumi signifikan Mw> 6.0 akibat aktivitas Sistem Busur Belakang Segmen Bali Lombok menggunakan analisis energi kumulatif dan periode ulang. *Jurnal Meteorologi dan Geofisika*, *21*(1), 29–35.

Halimatusadiyah, H., Suryanita, R., & Yusa, M. (2021). Evaluasi kinerja struktur bangunan beton bertulang di tanah khusus berdasarkan analisis pushover. *Racic : Rab Construction Research*, *6*(1), 39–47.

Hamdy, O., Gaber, H., Abdalzaher, M. S., & Elhadidy, M. (2022). Identifying exposure of urban area to certain seismic hazard using machine learning and GIS: A case study of greater Cairo. *Sustainability*, *14*(17), 10722.

Hariyanto, A. D., Triyadib, S., & Widyowijatnoko, A. (2022). A simple stilt structure technique for earthquake resistance of wooden vernacular houses in Bima, Sumbawa Island, Indonesia. *International Journal on Advanced Science, Engineering and Information Technology*, *12*(4), 1491–1497.

Hason, M. M., Hanoon, A. N., & Abdulhameed, A. A. (2021). Particle swarm optimization technique based prediction of peak ground acceleration of Iraq's tectonic regions. *Journal of King Saud University-Engineering Sciences*, 1–11.

Hsu, T.-Y., Wu, R.-T., Liang, C.-W., Kuo, C.-H., & Lin, C.-M. (2020). Peak ground acceleration estimation using P-wave parameters and horizontal-to-vertical spectral ratios. *Terrestrial, Atmospheric and Oceanic Sciences*, *31*, 1–8.

Imani, R., Arman, U. D., & Sari, A. (2021). The community capacity to respond to earthquakes and tsunami threat in Air Tawar Barat Sub-District, Padang City, West Sumatra, Indonesia. *IOP Conference Series: Earth and Environmental Science*, *708*(1), 12005. IOP Publishing.

Işık, E., Büyüksaraç, A., Ekinci, Y. L., Aydın, M. C., & Harirchian, E. (2020). The effect of site-specific design spectrum on earthquake-building parameters: A case study from the Marmara region (NW Turkey). *Applied Sciences*, *10*(20), 7247.

Jamil, M., Rahman, A. H. A., Siddiqui, N. A., Ibrahim, N. A., & Ahmed, N. (2020). A contemporary review of sedimentological and stratigraphic framework of the Late Paleogene deep marine sedimentary successions of West Sabah, North-West Borneo. *Bulletin of the Geological Society of Malaysia*, *69*(1), 53–65.

Karimzadeh, S., Feizizadeh, B., & Matsuoka, M. (2017). From a GIS-based hybrid site condition map to an earthquake damage assessment in Iran: Methods and trends. *International Journal of Disaster Risk Reduction*, *22*, 23–36.

Khoshnevis, N., Taborda, R., Azizzadeh-Roodpish, S., & Cramer, C. H. (2017). Seismic hazard estimation of northern Iran using smoothed seismicity. *Journal of Seismology*, *21*, 941–964.

Kowsari, M., Ghazi, H., Kijko, A., Javadi, H. R., & Shabani, E. (2021). Estimating the maximum earthquake magnitude in the Iranian Plateau. *Journal of Seismology*, *25*, 845–862.

Kumala, S. A., Huda, D. N., & Irawan, M. C. (2018). Analisis PGA (Peak Ground Acceleration) berdasarkan data gempa untuk wilayah Jakarta Timur menggunakan software PSHA. *Faktor Exacta*, *11*(4), 380–385.

Latifa, A., Meiliyadi, L. A. D., & Bahtiar, B. (2022). Analisis percepatan getaran tanah maksimum untuk memetakan kerawanan bencana gempa bumi dengan Metode Fukushima-Tanaka, Esteva dan Euclidean Distance di Pulau Lombok. *JIIF (Jurnal Ilmu Dan Inovasi Fisika)*, *6*(2), 123–130.

Linda, L., Ihsan, N., & Palloan, P. (2019). Analisis distribusi spasial dan temporal seismotektonik berdasarkan nilai b-value dengan menggunakan metode likelihood di Pulau Jawa. *Jurnal Sains dan Pendidikan Fisika*, *15*(1), 16–31.

Maringue, J., Mendoza, L., Sáez, E., Yañez, G., Montalva, G., Soto, V., … Sepúlveda, N. (2022). Geological and geotechnical investigation of the seismic ground response characteristics in some urban and suburban sites in Chile exposed to large seismic threats. *Bulletin of Earthquake Engineering*, *20*(10), 4895–4918.

Mase, L. Z. (2020). Seismic hazard vulnerability of Bengkulu City, Indonesia, based on deterministic seismic hazard analysis. *Geotechnical and Geological Engineering*, *38*(5), 5433–5455.

Mehta, P., & Thaker, T. P. (2022). Seismic hazard analysis of Vadodara region, Gujarat, India: Probabilistic & deterministic approach. *Journal of Earthquake Engineering*, *26*(3), 1438–1460.

Mendoza, R. B., Ramos, N., & Dimalanta, C. (2022). High-resolution peak ground acceleration modeling using geographic information systems: a case study of the potentially active Central Cebu Fault System, Philippines. *Journal of Asian Earth Sciences: X*, *7*(June), 100097.

Murdiantoro, R. A., Sismanto, S., & Marjiyono, M. (2018). Pemetaan daerah rawan kerusakan akibat gempabumi di Kotamadya Denpasar dan sekitarnya dengan menggunakan analisis mikrotremor, studi kasus : Gempabumi Seririt 14 Juli 1976. *Jurnal Fisika Indonesia*, *20*(2), 36–41.

Naik, N., & Choudhury, D. (2015). Deterministic seismic hazard analysis considering different seismicity levels for the state of Goa, India. *Natural Hazards*, *75*, 557–580.

National Agency for Disaster Management Australia-Indonesia Facility for Disaster Reduction. (2010). *Ringkasan hasil studi tim revisi peta gempa Indonesia 2010*.

Nicholson, U., Bray, V. J., Gulick, S. P. S., & Aduomahor, B. (2022). The Nadir Crater offshore West Africa: A candidate Cretaceous-Paleogene impact structure. *Science Advances*, *8*(33), eabn3096.

Noor, A. (2018). Perbandingan Algoritma support vector machine biasa dan support vector machine berbasis particle swarm optimization untuk prediksi gempa bumi. *Jurnal Humaniora Teknologi*, *4*(1), 31–37.

Pakpahan, S., Tambunan, M. P., Mannesa, M. D. M., & Tambunan, R. P. (2021). Pola spasial bahaya gempa bumi di sekitar bandara kertajati dan kesesuaiannya terhadap tata ruang wilayah. *Jurnal Geosaintek*, *7*(2), 73–82.

Pakuani, K. W., & Kurniawan, R. (2021). Kajian penentuan nilai epsilon optimal pada algoritma DMDBSCAN dan pemetaan daerah rawan gempa bumi di Indonesia Tahun 2014-2020. *Seminar Nasional Official Statistics*, *2021*(1), 991–1000.

Palupi, I. R., Raharjo, W., & Alfiani, O. D. (2020). Analisis guncangan gempa bumi Lombok dan Palu Tahun 2018. *Jurnal Lingkungan dan Bencana Geologi*, *11*(2), 87–96.

Pangaribuan, M. A., Rasimeng, S., Karyanto, K., & Rudianto, R. (2019). Analisis pendugaan bahaya kegempaan di batuan dasar untuk wilayah Lampung menggunakan Metode Psha. *JGE (Jurnal Geofisika Eksplorasi)*, *5*(3), 174–184.

Pasau, G., Bobanto, M. D., & Pandara, D. P. (2018). Model percepatan tanah maksimum di Kota Manado menggunakan Metode Donovan dan McGuire. *Jurnal MIPA*, *7*(1), 52–55.

Patel, M., Solanki, C., & Thaker, T. (2022). Deterministic seismic hazard analysis of Bharuch City and Surrounding Region. *Disaster Advances*, *15*(7), 27–33.

Pirhadi, N., Tang, X., & Yang, Q. (2019). New equations to evaluate lateral displacement caused by liquefaction using the response surface method. *Journal of Marine Science and Engineering*, *7*(2), 35.

Pouryari, M., Ardakani, A. R. M., & Hassani, N. (2022). A multi-criteria vulnerability of urban transportation systems analysis against earthquake considering topological and geographical method: A case study. *Iranian Journal of Science and Technology, Transactions of Civil Engineering*, *46*(3), 2147–2160.

Queirós, D., Calejo Rodrigues, R., & Pereira, N. (2016). Historical building acoustical retrofit: An experimental examination of traditional wooden floors. *Building Acoustics*, *23*(3–4), 181–191.

Rahman, R. R. A., & Wijayanto, A. W. (2021). Pengelompokan data gempa bumi menggunakan algoritma DBSCAN. *Jurnal Meteorologi dan Geofisika*, *22*(1), 31–38.

Resta, I. L., Apriliyani, D. P., Nasri, M. Z., & Dewi, I. K. (2021). Deterministic seismic hazard analysis for assessing earthquake hazard in Sungai Penuh and Kerinci Regency. *Journal of Physics: Conference Series*, *1876*(1), 12016. IOP Publishing.

Salahshoor, H., Lyubushin, A., Shabani, E., & Kazemian, J. (2018). Comparison of Bayesian estimates of peak ground acceleration (A max) with PSHA in Iran. *Journal of Seismology*, *22*, 1515–1527.

Salsabil, A. R., Hilyah, A., Purwanto, M. S., & Fajar, M. H. M. (2018). Zonasi bahaya kegempaan akibat patahan aktif di wilayah Jawa Timur dengan pendekatan deterministik menggunakan perhitungan Atenuasi Chiou-Youngs 2014 NGA. *Jurnal Geosaintek*, *4*(3), 103–112.

Sapanji, R., & Hamdani, D. (2020). Mapping of tsunami disaster mitigation evacuation routes of the movement of the Sunda Subduction Megathrust (case study: Coastal analysis of Southern Garut Regency). *Solid State Technology*, *63*(3), 2899–2911.

Sari, A. M., & Rahmatullah, F. S. (2021). Mapping of the peak ground acceleration and earthquake intensity In Padang City Using empirical formulation with accelerograph data validation. *Pillar of Physics*, *14*(2), 59–66.

Setyorini, A. (2020). Tingkat kesiapsiagaan kepala keluarga dalam menghadapi bencana gempa bumi di Kecamatan Pleret dan Piyungan Kabupaten Bantul. *Jurnal Kesehatan Al-Irsyad*, *13*(1), 84–92.

Shiuly, A. (2018). Global attenuation relationship for estimating peak ground acceleration. *Journal of the Geological Society of India*, *92*, 54–58.

Sinadinovski, C., Pekevski, L., Dojcinovski, D., & Cernih, D. (2018). Comparative analysis of strong motion (SM) records from the July 2017 Ohrid seismic sequence. *Journal of Seismology*, *22*, 1451–1467.

Somantri, O. (2021). Prediksi kekuatan gempa bumi Indonesia berdasarkan nilai magnitudo menggunakan Neural Network. *Prosiding Seminar Nasional Informatika Bela Negara*, *2*, 203–207.

Stewart, J. P., Luco, N., Hooper, J. D., & Crouse, C. B. (2020). Risk-targeted alternatives to deterministic ground motion caps in US seismic provisions. *Earthquake Spectra*, *36*(2), 904–923.

Sugino, M., Tanishima, W., Tanaka, K., Kashiwa, H., & Hayashi, Y. (2022). Effects of dynamic soil-structure interactions in an observed record on analyzing damages to wooden buildings in the 2016 Kumamoto Earthquake. *Journal of Structural Engineering B - J-STAGE*, *68B*, 408–414.

Sunardi, B., & Sulastri, S. (2016). Pemantauan anomali Total Electron Content (TEC) berkaitan dengan kejadian gempabumi di sekitar wilayah Jawa tahun 2015. *Spektra: Jurnal Fisika dan Aplikasinya*, *1*(2), 95–102.

Sung, C., Abrahamson, N. A., & Huang, J. (2021). Conditional ground-motion models for horizontal peak ground displacement for active crustal regions. *Bulletin of the Seismological Society of America*, *111*(3), 1542–1562.

Sungkowo, A. (2016). *Studi kerentanan seismik dan karakteristik dinamik tanah di Kota Yogyakarta dari data mikrotremor.*

Susilanto, P., Ngadmanto, D., Sunardi, B., & Rohadi, S. (2019). Analisis kecepatan gelombang geser (Vs) sebagai upaya mitigasi bencana gempabumi di Kulonprogo, DIY. *Jurnal Lingkungan dan Bencana Geologi*, *10*(2), 41–50.

Suwandi, E. A., Sari, I. L., & Waslaluddin, W. (2017). Analisis percepatan tanah maksimum, intensitas maksimum dan periode ulang gempa untuk menentukan tingkat kerentanan seismik di Jawa Barat (periode data gempa Tahun 1974-2016). *Wahana Fisika*, *2*(2), 12–30.

Syafitri, Y., Bahtiar, B., & Didik, L. A. (2020). Analisis pergeseran lempeng bumi yang meningkatkan potensi terjadinya gempa bumi di pulau Lombok. *Konstan - Jurnal Fisika dan Pendidikan Fisika*, *4*(2), 139–146.

Tauhidur, R., & Chhangte, R. L. (2021). *Estimation of Peak Ground Acceleration (PGA) and Spectral Acceleration (Sa) vertical component for interface subduction zone earthquakes of North-East India (NEI) and adjacent regions.*

The National Center for Earthquake Studies. (2017). *Peta sumber dan bahaya gempa Indonesia Tahun 2017*. Indonesia.

Tripathi, S., & Zafar, S. (2016). Deterministic seismic hazard analysis of the region. *International Journal of Engineering Research & Technology (IJERT)*, *5*(02), 634–636.

Ulfiana, E., Rumy, S. A., Pratama, R., & Ariy, P. (2018). Analisis pendekatan empiris PGA (Peak Ground Acceleration) Pulau Bali menggunakan Metode Donovan, MC. Guirre dan MV Mickey. *JIIF (Jurnal Ilmu dan Inovasi Fisika)*, *2*(2), 155–161.

Utomo, R. S., & Wahyudi, T. (2017). Kelayakan finansial Gua Jagung sebagai bioindustri di Kabupaten Bengkayang. *Jurnal Penelitian Dan Pengembangan Borneo Akcaya*, *4*(1), 1–15.

Verma, P., & Zafar, S. (2017). Comparative study on methodology of neo-deterministic seismic hazard analysis over DSHA and PSHA. *I-Manager's Journal on Structural Engineering*, *6*(4), 29–33.

Wang, F., Miyajima, M., Dahal, R., Timilsina, M., Li, T., Fujiu, M., … Zhao, Q. (2016). Effects of topographic and geological features on building damage caused by 2015.4. 25 Mw7. 8 Gorkha earthquake in Nepal: A preliminary investigation report. *Geoenvironmental Disasters*, *3*(1), 1–17.

Wibowo, N. B., & Sembri, J. N. (2016). Analisis Peak Ground Acceleration (PGA) dan intensitas gempabumi berdasarkan data gempabumi terasa Tahun 1981-2014 di Kabupaten Bantul Yogyakarta. *Indonesian Journal of Applied Physics*, *6*(01), 65–72.

Widagdo, A., & Permana, A. P. (2021). Extentional fault pada daerah compressive tectonic zone sebagai batas cekungan di Jawa Tengah Selatan. *Jambura Geoscience Review*, *3*(1), 40–45.

Yao, X., Qi, S., Liu, C., & Guo, S. (2021). An empirical attenuation model of the Peak Ground Acceleration (PGA) in the near field of a strong earthquake. *Natural Hazards*, *105*(1), 691–715. https://doi.org/10.1007/-s11069-020-04332-x

Yuliana, D. K., & Tejakusuma, I. G. (2016). Kemampuan penanganan terhadap ancaman bencana tsunami di wilayah pesisir kota Cilegon. *Jurnal Sains dan Teknologi Mitigasi Bencana*, *11*(1), 12–22.

Zera, T., Fauziah, A. R., Nafian, M., & Ramadhani, A. (2022). Mapping of Peak Ground Acceleration (PGA) values using the Donovan Model for Sumatran. *Journal of Physics: Conference Series*, *2243*(1), 12031. IOP Publishing.